Originalarbeit

Berg Huettenmaenn Monatsh (2024) Vol. 169 (3): 132–139
https://doi.org/10.1007/s00501-024-01428-w

BHM Berg- und Hüttenmännische Monatshefte

Impact Fracture Behaviour of Powder Metallurgy Steels Sintered at Different Temperatures

Milad Hojati, Christian Gierl-Mayer, and Herbert Danninger

Institut für Chemische Technologien und Analytik, Technische Universität Wien, Vienna, Austria

Received December 20, 2023; accepted January 6, 2024; published online January 22, 2024

Abstract: For powder metallurgy steels prepared through the press-and-sinter route, interparticle bonding is the most decisive feature defining the mechanical properties. It depends on the compacting pressure, but predominantly on the sintering conditions, mainly the sintering temperature. In the present contribution, the progressive strengthening of the sintering necks with increasing temperature is shown by fractography for plain carbon steels as well as alloyed grades. For sintered steels, in contrast to wrought steels, the appearance of cleavage fracture is rather a positive sign, indicating pronounced interparticle strength as attained at high sintering temperatures. At lower temperatures, in contrast, localised failure of the sintering necks typically occurs as ductile rupture, but with rather low consumed energy. Alloy elements with a high oxygen affinity introduced by prealloying retard formation of sound sintering bridges up to temperatures at which carbothermal reduction of the surface oxides becomes possible, while admixing such elements through suitable masteralloys yields attractive interparticle strength already at standard belt furnace temperatures of 1120 °C.

Keywords: Powder metallurgy, Sintered steels, Impact testing, Fractography

Einfluss der Sintertemperatur auf das Schlagbruchverhalten von pulvermetallurgischen Stählen

Zusammenfassung: Bei pulvermetallurgischen Stählen, die durch Pressen und Sintern hergestellt werden, ist der Teilchenverbund der wichtigste Parameter für die mechanischen Eigenschaften. Er hängt vom Pressdruck und den Sinterbedingungen ab, vor allem der Temperatur. In diesem Beitrag wird die Festigkeitszunahme mit steigender Temperatur durch fraktographische Untersuchungen an Fe-C sowie an legierten Varianten gezeigt. Im Gegensatz zu schmelzmetallurgischen Stählen ist bei Sinterstählen das Auftreten von Spaltbruch ein positives Signal, weil es hohe Festigkeit der Sinterkontakte anzeigt, wie das durch hohe Sintertemperaturen erreicht wird. Bei niedrigeren Temperaturen tritt der Bruch lokalisiert an den Sinterkontakten auf, zwar duktil, aber mit geringem Energieverbrauch. Sauerstoffaffine Legierungselemente, die vorlegiert eingebracht werden, erfordern für die Bildung stabiler Sinterkontakte Temperaturen, bei denen eine carbothermische Reduktion der Oberflächenoxide möglich wird. Ein Zusatz solcher Elemente über die Masteralloy-Route dagegen ergibt gute Versinterung schon bei den üblichen Bandofentemperaturen um 1120 °C.

Schlüsselwörter: Pulvermetallurgie, Sinterstähle, Schlagbiegeversuch, Fraktographie

1. Introduction

Powder metallurgy (PM) precision parts produced by the press-and-sinter route have found increasing applications, mainly in conventional automotive drivetrain systems, i.e. combustion engines and transmissions [1]. With the trend to alternative drivetrains, new applications for ferrous powder metallurgy parts have to be identified [2]. This requires improved mechanical properties; new alloying systems are needed, since the traditional alloy elements in high strength sintered steels, Cu and Ni, suffer from recycling and health hazard problems; furthermore, the demand for these elements will increase in the future, and thus also the price, because of their increased use in electromobility, energy systems, and more. Therefore, the use of cheaper alloy elements, such as Cr, Mn, and Si, is desirable to offset the penalty of the PM route caused by alloying cost [3].

The main difference between classical wrought steels and sintered steels is the inherent porosity of the latter, caused by the fact that cold uniaxial compaction at industrially feasible pressures can yield relative density levels

H. Danninger (✉)
Institut für Chemische Technologien und Analytik,
Technische Universität Wien,
Getreidemarkt 9/164-03-3,
1060 Vienna, Austria
herbert.danninger@tuwien.ac.at

of 88 to 92% maximum [4, 5]. This density level does not change markedly during sintering, since densification during sintering, which is standard requirement for production of hardmetals or tungsten heavy alloys, is undesirable for ferrous precision parts because of negative effects on the geometrical precision. These parts thus contain typically a porosity of between 8 and 12%, which adversely affects the mechanical strength [6, 7] but, on the other hand, improves the noise damping capacity [8] and renders the steels insensitive to overheating during heat treatment [9].

At the porosity levels mentioned above, the pores are interconnected and usually open to the surface [10]. I.e. the structure of the material is "sponge-like", containing in principle one single complex shaped pore [11] and not like the "Swiss cheese" model in which the pores are present as isolated cavities. Interconnected porosity, however, means that the sintering contacts between the powder particles are isolated, and the properties, mechanical ones but also thermal and electrical conductivity, are decisively controlled by the quality of the contacts [12]. Therefore, the development of these interparticle necks, from pressing contacts in the pressed ("green") state to solid metallic bridges, is highly relevant for predicting the properties of sintered steel parts. The localization of the stresses to the interparticle regions also implies that the fracture behaviour cannot be directly compared to that of fully dense wrought steels, even of the same composition.

Fractography is an excellent tool for investigating the quality of the sintering contacts [13]. In the present study, the development of the contacts as a function of the sintering temperature has been investigated for different types of PM steels through studying the impact fracture behaviour, the Charpy impact test being the most severe mechanical test for the quality of interparticle strength in sintered steels.

TABLE 1
Composition of the powder mixes (in mass%)

Code	Cr	Mo	Mn	Si	$C_{nominal}$	Fe
Fe-C	0.0	0.0	0.0	0.0	0.8	Balance
AstMo	0.0	1.5	0.0	0.0	0.8	Balance
AstCrM	3.0	0.5	0.0	0.0	0.8	Balance
Masteralloy	0.0	0.0	1.6	0.3	0.8	Balance

2. Experimental Procedure

The starting powders used were plain iron powder ASC100.29, Mo prealloyed steel powder Astaloy Mo as well as Cr-Mo prealloyed powder Astaloy CrM (all from Höganäs AB, Sweden). Natural graphite UF4 (Kropfmühl) was admixed as carbon carrier, and for one steel grade, an ultra high pressure water atomized masteralloy powder (Atomising Systems Ltd., Sheffield) was added. The compositions studied are given in Table 1; it should be noted that the carbon content given is the nominal one, i.e. the admixed graphite, while, in the as sintered state, the C level ("C combined") is typically lower, as a consequence of carbothermal reduction of the oxides present in the starting powders.

The powders were mixed in a Turbula mixer and compacted at 600 MPa in a pressing tool with floating die to Charpy impact test bars ISO5754. Die wall lubrication was afforded using Multical sizing fluid to avoid undesirable effects by admixed lubricant. The pressed compacts were

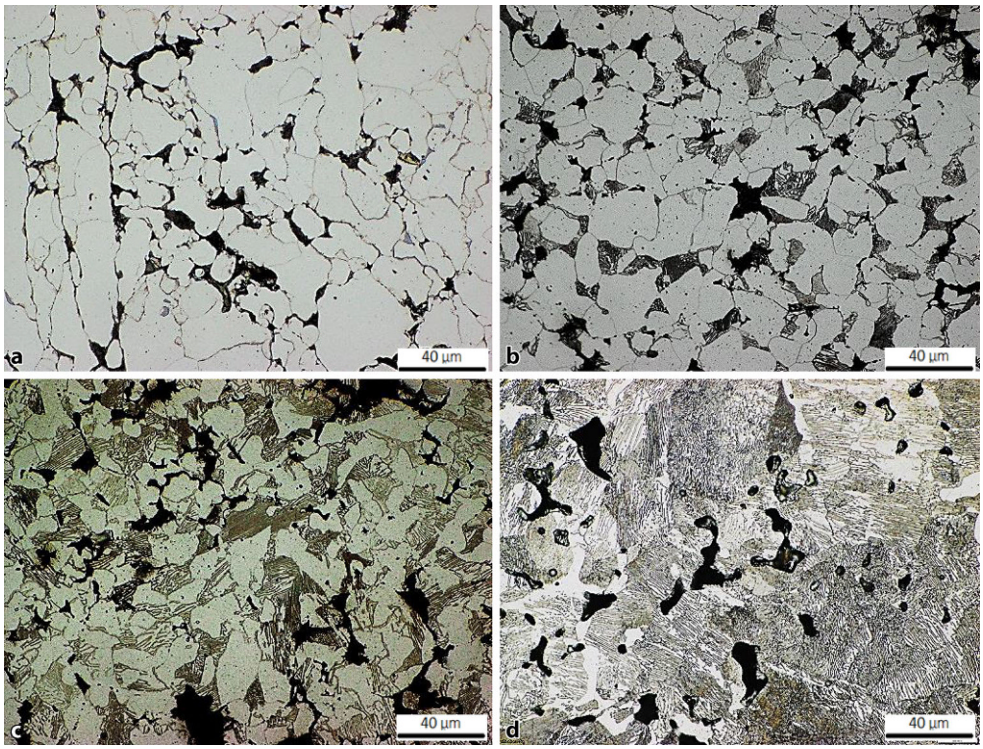

Fig. 1: Micrographs of carbon steel Fe-0.8%$C_{nominal}$, compacted at 600 MPa, sintered 60 min at varying temperatures in Ar. Nital etched. **a** 700 °C; 64 HV30; 0.786%C_{comb}. **b** 900 °C; 79 HV30; 0.776%C_{comb}. **c** 1000 °C; 103 HV30; 0.752%C_{comb}. **d** 1300 °C; 134 HV30; 0.733%C_{comb}

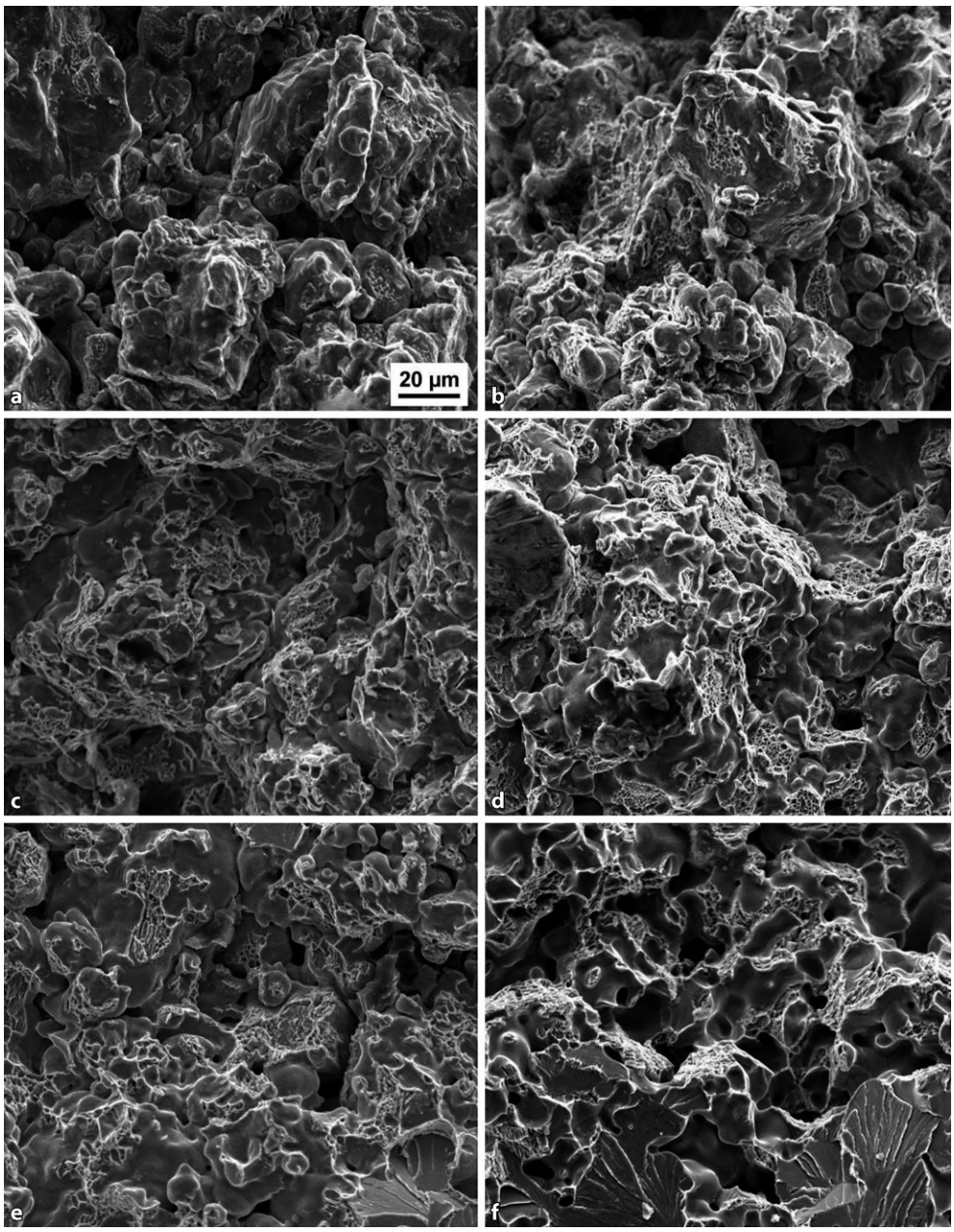

Fig. 2: Impact fracture surfaces of carbon steel Fe-0.8%$C_{nominal}$, compacted at 600 MPa, sintered 60 min at varying temperatures in Ar. 1000×. **a** 700 °C; IE = 0.5 J.cm^{-2}, O content 0.11%. **b** 800 °C; IE = 5.3 J.cm^{-2}, O content 0.09%. **c** 900 °C; IE = 9.7 J.cm^{-2}, O content 0.08%. **d** 1000 °C; IE = 14.5 J.cm^{-2}, O content 0.04%. **e** 1100 °C; IE = 17.2 J.cm^{-2}, O content 0.02%. **f** 1300 °C; IE = 26.0 J.cm^{-2}, O content 0.004%

sintered for 60 min in an electrically heated furnace with superalloy retort, the temperature being varied between 700 and 1300 °C. The atmosphere was argon of 99.999% purity. The boat containing the specimens was directly pushed into the hot zone of the furnace, and after the isothermal period the boat was pushed into the water jacketed exit zone of the furnace, cooling at a (linearized) rate of about 25 K/min.

The specimens were impact tested according to ISO5754, i.e. unnotched and perpendicular to the pressing direction, and the fracture surfaces were characterized by SEM (FEI Quanta 200) in SE mode. To investigate esp. the effect of carbon dissolution, metallographic cross sections were prepared, and the hardness was measured on the sections. The combined carbon content of the sintered specimens was measured by combustion analysis (LECO CS-230) and the total oxygen content by hot fusion analysis (LECO TC-400).

3. Unalloyed Carbon Steel

In a first test series, plain carbon steel was investigated. In the microstructures (Fig. 1), the most evident effect is the increase of the pearlite content, as a consequence of progressive carbon dissolution. This is a self-sustaining process since carbon pickup enhances the ferrite-austenite transformation, which in turn results in increased solubility of carbon. Nevertheless, the main dissolution process occurs between 900 and 1000 °C [14], either through solid state reaction [15] or the gas phase [16], as is also visible

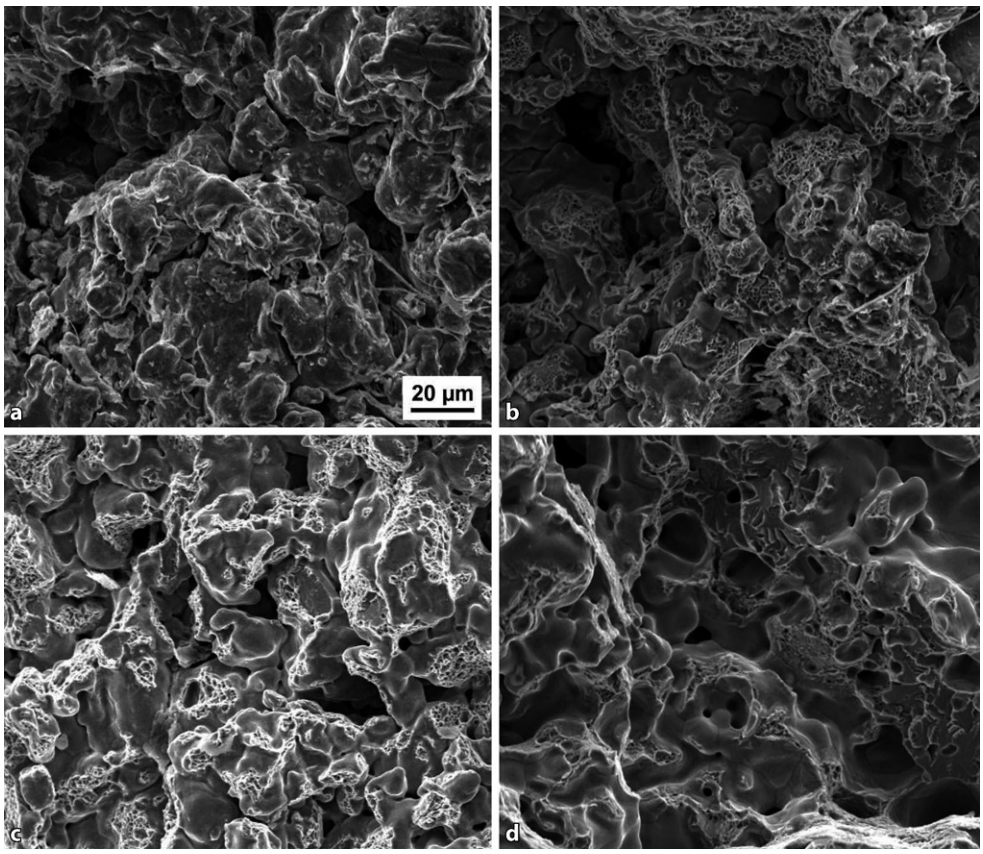

Fig. 3: Impact fracture surfaces of Mo prealloyed Fe-1.5%Mo-0.8%$C_{nominal}$, compacted at 600 MPa, sintered 60 min at varying temperatures in Ar. 1000 ×. **a** 700 °C; IE = 0.2 J.cm^{-2}; O content 0.11%. **b** 900 °C; IE = 3.6 J.cm^{-2}; O content 0.08%. **c** 1000 °C; IE = 7.0 J.cm^{-2}; O content 0.04%. **d** 1300 °C; IE = 16.4 J.cm^{-2}; O content 0.01%

from the increased hardness, despite slightly lower total carbon content.

In Fig. 2 the impact fracture surfaces are shown. In the specimens sintered at 700 °C, there is virtually no sign of interparticle contacts, which agrees with the very low impact energy. At 800 °C, slight ridges and miniature dimples are visible, indicating ductile failure of very small localized metallic contacts. At 900 °C, the broken contacts are more prominent, and their total area is significantly larger; a further increase of the total contact area is visible at 1000 °C, but the broken contacts still show dimples. At 1100 °C, once more ductile fracture is prominent, but there are some cleavage areas. At still higher temperatures, the dimples are further enlarged, and there are more and larger cleavage areas.

If the morphology of the fracture surfaces is compared with the impact energy data, it stands out clearly that the emergence of cleavage fracture is not related to a decrease of the impact energy. This can be related to the specific microstructure and resulting fracture mode: as stated above, in sintered steels containing interconnected porosity, mechanical loading—and thus plastic deformation—is concentrated at the sintering contacts. Vedula and Heckel [12] stated that the energy consumed during fracture is related to the deformed volume, which is increased when the sintering contacts are enlarged. If the contacts are sufficiently strong, a crack that may be initiated at sintering contacts may proceed through the cores of the original powder particles, at least if the pearlite lamellae are suitably oriented. Therefore the emergence of cleavage fracture in sintered steels can be regarded as an indicator that the sintering process has been effective to a degree that the sintering necks are not necessarily the predetermined locations for failure any more. Surely, ductile failure of the sintering necks, as indicated by dimple structures, consumes relatively more energy that cleavage fracture, but if the contacts are small, the deformed volume is small, too, and such is the consumed energy.

4. Sintered Alloy Steels

In sintered alloy steels, also the effect of the alloy elements on sintering and resulting deformation behaviour must be considered. For powder metallurgy steels, the way to introduce alloy elements is a further parameter, since there are different alloying routes, admixing—as is done with graphite—, prealloying, in which the alloy elements are introduced into the melt from which the powder is atomized, or the "masteralloy" approach which uses admixed powder which, however, contains several alloy elements in one [17, 18]. This latter route offers the chance to tailor the composition of the masteralloy such that its melting range is below the isothermal sintering temperature [19]. Thus, a transient liquid phase is formed in the early stage of sintering which strongly enhances the distribution of the alloy elements in the ferrous matrix.

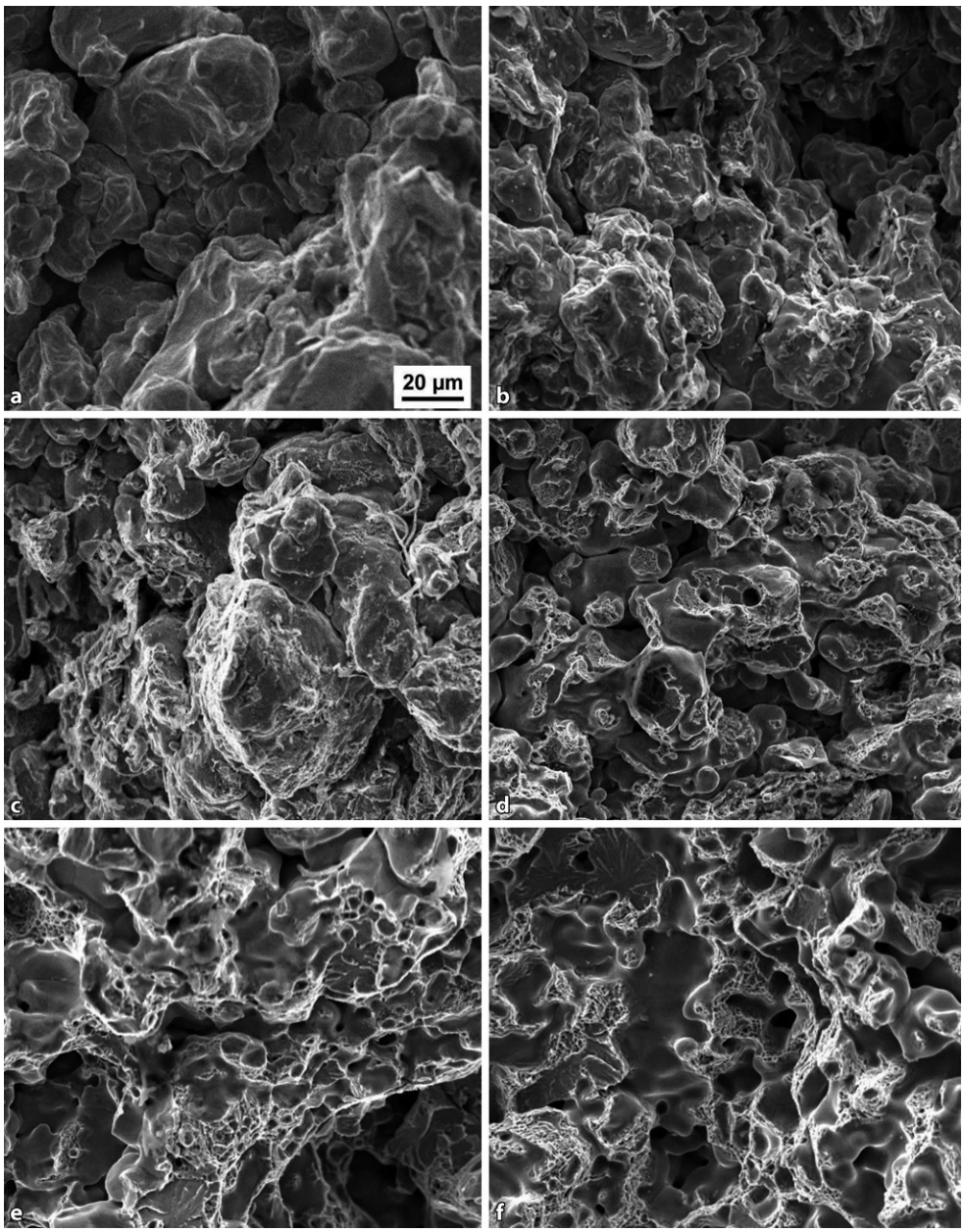

Fig. 4: Impact fracture surfaces of Cr-Mo prealloyed Fe-3.0%Cr-0.5%Mo-0.8%$C_{nominal}$, compacted at 600 MPa, sintered 60 min at varying temperatures in Ar. 1000 ×. **a** 700 °C; IE = 0.1 J.cm^{-2}; O content 0.22%. **b** 900 °C; IE = 0.5 J.cm^{-2}, O content 0.22%. **c** 1000 °C; IE = 3.4 J.cm^{-2}, O content 0.17%. **d** 1100 °C; IE = 8.9 J.cm^{-2}, O content 0.12%. **e** 1200 °C; IE = 16.7 J.cm^{-2}, O content 0.03%. **f** 1300 °C; IE = 20.1 J.cm^{-2}, O content 0.01%

In the present study, different alloy elements as well as alloying variants were included. One steel grade was prepared from Mo prealloyed powder; Mo is similar to Fe regarding the stability of the oxides. A further variant was based on Cr-Mo prealloyed powders; here, the fairly stable Cr oxides at the particle surfaces have been shown to inhibit sintering unless the sintering temperatures are sufficiently high to enable carbothermal reduction of these oxides [20–23]. Finally, a masteralloy variant using an ultra high pressure water atomized powder (Fe-40%Mn-6.7%Si-0.5%C, 2.18%O, $d_{50,3}$ = 6.7 µm) as alloy element carrier was prepared [24]. These alloy elements are also sensitive to oxygen, but the chemical activity is significantly lower in the masteralloy than e.g. in elemental powders.

Test specimens were prepared and tested as shown above.

In Fig. 3, fracture surfaces of the Mo prealloyed steel are shown. Evidently the fracture morphology is rather similar to that of the plain carbon steel at the same temperature, with progressive formation and growth of the sintering contacts with higher temperature, the contacts failing through ductile rupture. Above 1100 °C, also cleavage facets are visible. This is not surprising, since, as stated above, deoxidation of the Mo alloyed powder particles occurs in a similar way as with plain iron since the stability of Mo oxides is rather similar to that of iron oxides; the as-sintered oxygen contents given also are similar for both materials. The emergence of cleavage facets once more indicates sound interparticle contacts. While in case of plain carbon steels the orientation of the lamellae in pearlite defines cleavage,

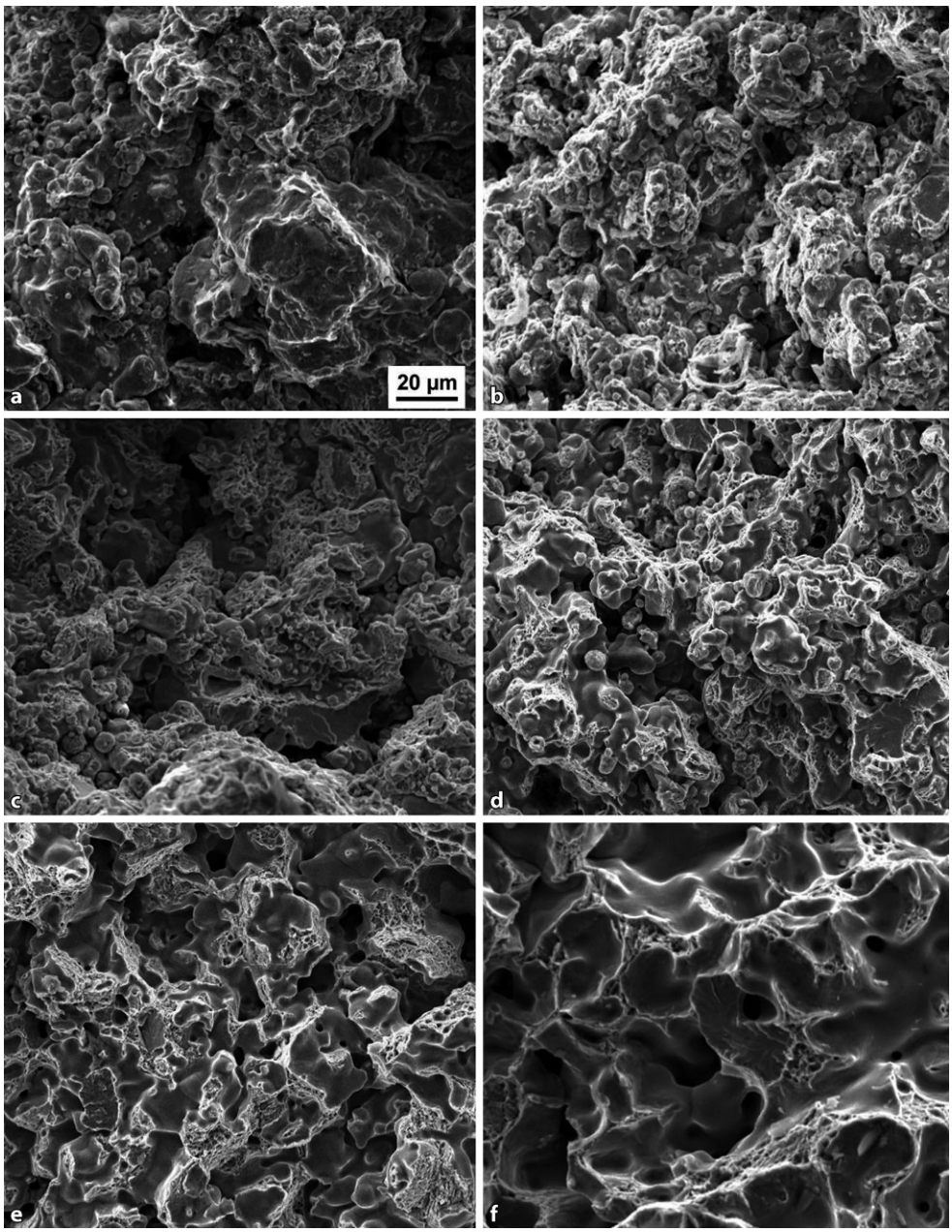

Fig. 5: Impact fracture surfaces of Fe-1.6%Mn-0.3%Si-0.8% $C_{nominal}$ (4% Mn-Si masteralloy), compacted at 600 MPa, sintered 60 min at varying temperatures in Ar. 1000×. **a** 700 °C; IE = 0.3 J.cm^{-2}; O content 0.28%. **b** 800 °C; IE = 5.4 J.cm^{-2}, O content 0.20%. **c** 900 °C; IE = 8.6 J.cm^{-2}, O content 0.20%. **d** 1000 °C; IE = 10.6 J.cm^{-2}, O content 0.19%. **e** 1100 °C; IE = 21.5 J.cm^{-2}, O content 0.07%. **f** 1300 °C; IE = 33.7 J.cm^{-2}, O content 0.01%

in Mo alloyed steels it is the coarse upper bainite typical for as sintered microstructures. The lower maximum impact energy recorded here as compared to Fe-C can be related to the markedly higher (apparent) hardness, 185 HV30 compared to 134 HV30 after sintering at 1300 °C, which of course lowers the ductility.

Figure 4 depicts the fractographs of the steel specimens prepared from the Cr-Mo prealloyed powder. Here the morphologies are markedly different from that of the previously shown materials: Not only at 700 °C sintering temperature but also up to 900 °C, there are virtually no signs of interparticle contacts; the particles pressed together have separated without any plastic deformation. At 1000 °C, the first very small broken contacts are visible, which with the previously shown materials were present already at 800 °C. Starting from 1100 °C, clearly defined sintering contacts are found that have failed in a ductile manner, but still with very fine dimples, and above this temperature the fracture surfaces resemble those of Fe-C and Fe-Mo-C sintered at equivalent temperature, with ductile fracture and coarse dimples as well as some cleavage facets. This appearance of the fracture surfaces agrees well with the impact energy data, the values being marginal at 700 up to 900 °C and still low at 1000 °C, acceptable at 1100 °C, while sound data are recorded at 1200 and 1300 °C.

The reason for this different behaviour is found in the oxygen contents. As stated above, the Cr containing prealloyed powders are covered with oxide layers that are much more stable thermodynamically than oxides containing only Fe and/or Mo. Stable oxides require higher tem-

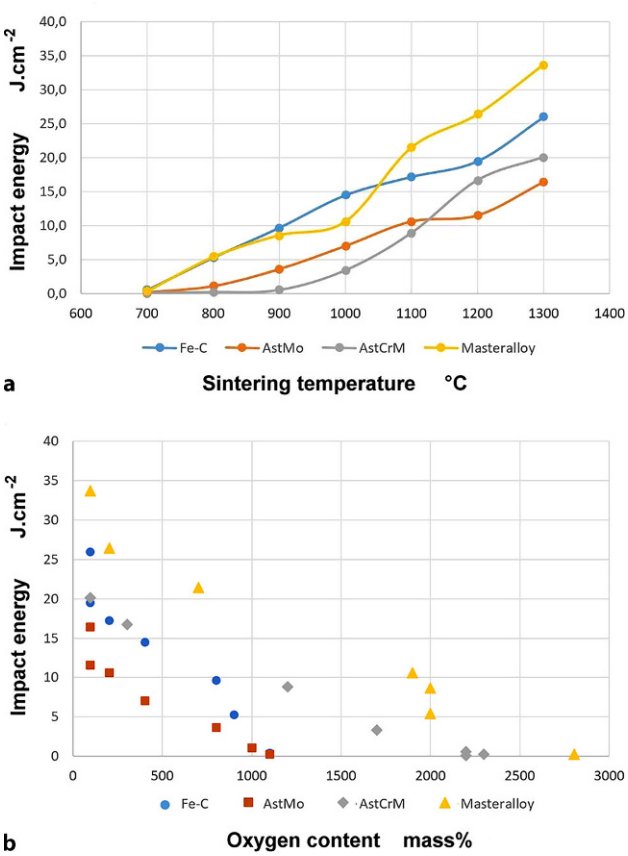

Fig. 6: **a** Impact energy (unnotched) vs. sintering temperature. **b** Impact energy (unnotched) vs. oxygen content

peratures for carbothermal reduction; as shown e.g. in [22], the surface oxides of Fe-C or Fe-Mo-C are carbothermally removed in the temperature range of 700 to 800 °C and of the Cr-Mo steels at 1000 to 1100 °C, and for those oxides enclosed in the powder particles and the pressing contacts the temperature "windows" are 900 to 1100 °C and 1100 to 1250 °C, respectively. This agrees well with the oxygen data given in Fig. 4, which show that attaining really low oxygen contents requires temperatures of 1200 °C and above, the oxygen-free sintering contacts then resulting in accordingly high impact energy data which, combined with the high apparent hardness of 330 HV30 after sintering at 1300 °C, confirm the high potential of these steels when sintered at suitably high temperatures.

Figure 5 depicts fractographs of specimens prepared with the Mn-Si masteralloy. This alloying technique is similar to the mixing route through which graphite is added, but it is similar to the previously described material, since it contains alloy elements with fairly high oxygen affinity, both Mn and Si forming oxides that are more stable than even those of Cr. In contrast to the Cr-Mo-steel, however, the fracture surfaces show plastically broken sintering necks even at as low as 800 °C, similar to Fe-C and Fe-Mo-C. With increasing temperature, the areas showing ductile failure progressively increase, and the dimples grow, indicating higher plasticity. At 1200 and 1300 °C, the fracture surfaces resemble those attained with the Cr-Mo steel.

The fracture surfaces are in good agreement with the impact energy data, which for this variant are measurable already at sintering temperatures below 1000 °C, and at 1100 °C, >20 J.cm^{-2} are attained (Fig. 6a), which is a highly attractive value for a sintered alloy steel. After sintering at 1300 °C, even >30 J.cm^{-2} are recorded, at an apparent hardness close to 200 HV30. There is, however, a disagreement between the impact energy data and the oxygen content: while with all other materials the impact energy is the higher the lower the oxygen content is, with the masteralloy grade reasonable impact energy data are attained even at oxygen levels >0.1%, as shown in Fig. 6b.

The reason for this surprising behaviour can be found in the "internal getter" effect, which means oxygen transfer from a base powder containing oxides with low stability to alloy element particles with high oxygen affinity [25]. This occurs in powder compacts since in the temperature range 700 to 1000 °C the local atmosphere in the pore network is reducing for iron oxides but is strongly oxidizing for elements such as Mn or Si. Therefore, during heating of the powder compact, the surfaces of the base powder particles are reduced carbothermally, forming CO, but this is immediately gettered by the masteralloy particles, oxidizing them, and the net reaction is in fact a metallothermic reduction of the iron oxides. This results in a pronounced cleaning of the iron particles and in high sintering activity, which explains why significant interparticle bonding is observed at rather low temperatures.

The oxygen bonded to the masteralloy particles is not too detrimental to the mechanical properties, as indicated e.g. by the material sintered at 1100 °C, which contains 700 ppm oxygen but nevertheless shows an impact energy of >20 J.cm^{-2}. Removal of the stable Mn and Si oxides requires temperatures of at least 1200 °C, which further improves the mechanical properties. These results show that it is not only the total oxygen content but also the oxygen distribution that controls the mechanical properties: oxides evenly present at the base powder surfaces (or at the grain boundaries of sintered specimens [26]) are more detrimental than oxides that are enriched just locally.

In any case, however, the masteralloy approach seems to be attractive for introducing alloy elements with high oxygen affinity into PM steel parts that are sintered in standard mesh belt furnaces at temperatures in the range 1100 to 1130 °C, which are definitely too low for the otherwise highly promising Cr prealloyed grades.

5. Conclusions

The formation and growth of interparticle contacts in ferrous powder compacts is strongly affected by the sintering temperature but also by the composition of the steels, and in case of alloy steels, by the elements added and the alloying route chosen. With Fe-C and Fe-Mo-C, i.e. in material systems that do not contain elements with high oxygen affinity, formation of small, localized sintering contacts are observed at temperatures as low as 800 °C, and the contacts grow with higher sintering temperatures. The fractographs show ductile rupture of the necks, and at sintering temper-

atures of 1100 °C and above, also cleavage facets emerge, indicating strong interparticle contacts. Therefore, in contrast to wrought steels, cleavage facets are rather a positive sign, indicating that the sintering contacts are sufficiently strong so that the crack is deflected into the core of the powder particles at least locally.

For steels alloyed with elements of high oxygen affinity, the effect of the temperature strongly depends on the alloying route. In case of prealloying with Cr, poor interparticle bonding was observed up to at least 1000 °C because the surface oxides prevent formation of stable metallic contacts. However, in case of sintering temperatures at which carbothermal reduction of the Cr oxides becomes effective, excellent combinations of hardness and impact energy are recorded. When introducing Mn and Si through a suitable masteralloy, formation of contacts occurs at a similar stage as for Fe-C, despite the presence of these oxygen-affine elements and despite rather high oxygen content. This can be related to the "internal getter" effect, which results in cleaning the surfaces of the base iron powder particles and according activation of sintering, the oxygen being transferred to the masteralloy particles. Removal of the oxygen thus bonded requires temperatures at and above 1200 °C, but even at 1100 °C, attractive properties are obtained. From the practical viewpoint, this means that, if sintering is to be done in belt furnaces, the masteralloy approach is to be preferred, while if high temperature furnaces are available, both the masteralloy route and Cr prealloying are promising.

Acknowledgements. The authors want to thank Miba Sinter Austria GmbH, Vorchdorf, for supplying most of the powders used, and Atomising Sytems Ltd., Sheffield, UK, for producing and supplying the masteralloy powders.

Funding. Open access funding provided by TU Wien (TUW).

References

1. Whittaker, D.: Powder Metall. Review 4. No **2**, 35–53 (2015)
2. Kotthoff, G., Leupold, B., Janzen, V.: Pulvermetallurgie in Wissenschaft und Praxis, vol.33, Fachverband Pulvermetallurgie, Hagen, pp. 185–206 (2017)
3. Arnhold, V., Kruzhanov, V.: Pulvermetallurgie in Wissenschaft und Praxis, vol.36, Fachverband Pulvermetallurgie, Hagen, pp. 233–252 (2021)
4. Schatt, W., Wieters, K.-P., Kieback, B. (ed.), in: Pulvermetallurgie. 2nd Ed., Springer, (2007)
5. Šalak, A.: Ferrous Powder Metallurgy. Cambridge Int. Sci. Publ, Cambridge UK (1995)
6. Haynes, R.: Mechanical properties of sintered metals. Freund Publishers London UK (1981)
7. Danninger, H., et al.: powder metall. Int **25**(170–173), 219–223 (1993)
8. Hellein, R., et al.: Pulvermetallurgie in Wissenschaft und Praxis, vol.35, Fachverband Pulvermetallurgie, Hagen, pp. 33–50 (2019)
9. Dlapka, M., et al.: Pract.Metallogr. 47. No **2**, 686–699 (2010)
10. Dlapka, M., et al.: Metal Powder Report. No **2**, 30–33 (2010)
11. Danninger, H., et al.: Pract. Metallogr. 31. No **2**, 56–69 (1994)
12. Vedula, K., Heckel, R.W.: Modern Dev. Powder Met. **12**, 759–775 (1981)
13. Dudrova, E., Kabatova, M.: Powder Met. **59**, 148–167 (2016)
14. Danninger, H., Frauendienst, G.: Mat. Chem Phys , 72–77 (2001)
15. Dautzenberg, N., Hewing, J.: Powder Metall. Int. **9**(1), 16–19 (1977)
16. Tanaka, Y., Lund, J.: Int. J. Powder Met. **22**(2), 73–80 (1986)
17. Zapf, G., Dalal, K.: Modern Dev. Powder Met. **10**, 129–152 (1977)
18. Schlieper, G., Thümmler, F.: Powder Metall. Int. 11. No **4**, 172–176 (1979)
19. de Oro Calderon, R., et al.: Powder Metall. 60. No **2**, 86–96 (2017)
20. Castro, F., Ortiz, P.: Proc. EuroPM2003, Valencia. EPMA, Shrewsbury UK **1**, 261–268 (2003)
21. Ortiz, P., Castro, F.: Powder Metall. 47. No **3**, 291–298 (2004)
22. Danninger, H., et al.: Powder Metall. Progress 2. No **3**, 125–140 (2002)
23. Kremel, S., et al.: Powder Metall. Progress 2. No **4**, 211–221 (2002)
24. Hojati, M., Gierl-Mayer, C., Danninger, H.: Metals **12**, 13 (2022)
25. Gierl-Mayer, C., et al.: JOM **68**(3), 920–927 (2016)
26. Hryha, E.: Fundamental study of Mn containing PM steels with alloying method of both premix and pre alloy. PhD thesis, Slovak Academy of Sciences, Kosice (2007)